

Tuning the lability of a series of Ru(II) polypyridyl complexes: a comparison of experimental-kinetic and DFT-predicted reaction mechanisms

Dušan Čoćić , Marta Chrzanowska , Anna Katafias , Ralph Puchta & Rudi van Eldik

To cite this article: Dušan Čoćić , Marta Chrzanowska , Anna Katafias , Ralph Puchta & Rudi van Eldik (2021): Tuning the lability of a series of Ru(II) polypyridyl complexes: a comparison of experimental-kinetic and DFT-predicted reaction mechanisms, Journal of Coordination Chemistry, DOI: [10.1080/00958972.2021.1874369](https://doi.org/10.1080/00958972.2021.1874369)

To link to this article: <https://doi.org/10.1080/00958972.2021.1874369>



Published online: 19 Jan 2021.



Submit your article to this journal [↗](#)




View related articles [↗](#)



View Crossmark data [↗](#)



Tuning the lability of a series of Ru(II) polypyridyl complexes: a comparison of experimental-kinetic and DFT-predicted reaction mechanisms

Dušan Čočić^a, Marta Chrzanowska^b, Anna Katafias^b, Ralph Puchta^{c,d,e}  and Rudi van Eldik^{b,c,f}

^aDepartment of Chemistry, Faculty of Science, University of Kragujevac, Kragujevac, Serbia; ^bFaculty of Chemistry, Nicolaus Copernicus University in Toruń, Toruń, Poland; ^cInorganic Chemistry, Department of Chemistry and Pharmacy, University of Erlangen-Nuremberg, Erlangen, Germany; ^dComputer Chemistry Center, Department of Chemistry and Pharmacy, University of Erlangen-Nuremberg, Erlangen, Germany; ^eCentral Institute for Scientific Computing (ZISC), University of Erlangen-Nuremberg, Erlangen, Germany; ^fFaculty of Chemistry, Jagiellonian University, Krakow, Poland

ABSTRACT

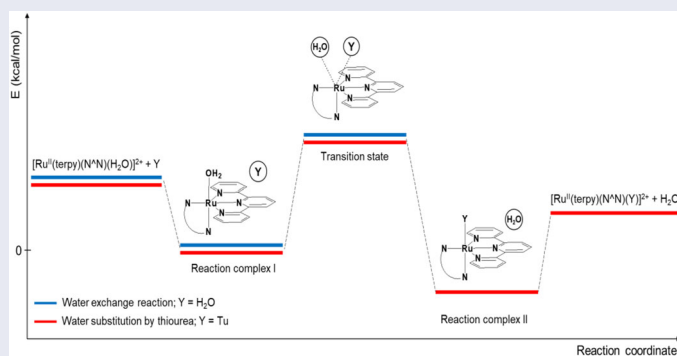
This report deals with a comparison of experimentally obtained kinetic and activation parameter data, and theoretical DFT computations, in terms of mechanistic information on the water exchange and water displacement reactions by thiourea for a series of complexes of the type $[\text{Ru}^{\text{II}}(\text{terpy})(\text{N}^{\wedge}\text{N})(\text{H}_2\text{O})]^{2+}$, where terpy = 2,2':6',2''-terpyridine and $\text{N}^{\wedge}\text{N}$ represents ethylenediamine (en), 2-(aminomethyl)pyridine (ampy), 2,2'-bipyridine (bipy), 1,10-phenanthroline (phen), and $\text{N},\text{N},\text{N}',\text{N}'$ -tetramethylethylenediamine (tmen). The complexes were all isolated in the form of $[\text{Ru}(\text{terpy})(\text{N}^{\wedge}\text{N})\text{Cl}]\text{X}$ ($\text{X} = \text{Cl}^-$ or ClO_4^-) compounds and fully characterized in both the solid state and in solution. The DFT calculations revealed further mechanistic insight into the water exchange reactions as well as the water displacement reactions by thiourea. Both the experimental activation parameters and the DFT calculations suggest the operation of an associative interchange (I_a) mechanism for both reaction types studied.

ARTICLE HISTORY

Received 5 November 2020
Accepted 4 January 2021

KEYWORDS

Kinetic data; ligand substitution; water exchange reactions; Ru(II) polypyridyl complexes; DFT calculations; mechanistic insight



CONTACT Ralph Puchta  ralph.puchta@fau.de; Rudi van Eldik  rudi.vaneldik@fau.de  Inorganic Chemistry, Department of Chemistry and Pharmacy, University of Erlangen-Nuremberg, Erlangen, Germany.

Dedicated to Jerry Atwood in recognition of his numerous contributions to Metallosupramolecular Complexes.

© 2021 Informa UK Limited, trading as Taylor & Francis Group

Introduction

The goal of this article is to compare the mechanistic insight gained from classical kinetic studies with that obtained from DFT calculations. In this report, mechanistic studies on a group of Ru(II) polypyridyl complexes with diverse electronic properties (σ donor and π back-bonding) and steric hindrance were made possible through the selection of suitable spectator ligands. A series of five polypyridyl Ru(II) complexes of the type $[\text{Ru}(\text{terpy})(\text{N}^{\wedge}\text{N})\text{Cl}]\text{X}$ ($\text{terpy} = 2,2':6',2''\text{-terpyridine}$, $\text{N}^{\wedge}\text{N} = \text{bidentate N,N-donor ligand}$, $\text{X} = \text{Cl}^-$ or ClO_4^-) with different bidentate spectator ligands: ethylenediamine (en), **1**, 2-(aminomethyl)pyridine (ampy), **2**, 2,2'-bipyridine (bipy), **3**, 1,10-phenanthroline (phen), **4**, and N,N,N',N'-tetramethylethylenediamine (tmen), **5**, were synthesized. The complexes, schematically presented in Figure 1, were fully characterized in the solid state by single crystal X-ray diffraction and elemental analysis, as well as in solution applying ESI-mass spectrometry, and NMR and electronic absorption spectroscopies [1–4]. The coordination sphere consists of a tridentate π -acceptor terpyridine chelate, a bidentate ligand of diverse electronic and steric properties, and a chlorido ligand. These complexes were employed to study their aquation reactions and chemical behavior in terms of ligand substitution reactions with chloride and thiourea. All reactions were followed using electronic absorption spectroscopy in the visible range under pseudo-first-order conditions, i.e. using at least a 10-fold excess of the entering ligand over the Ru(II) concentration. The results of these mechanistic studies are now

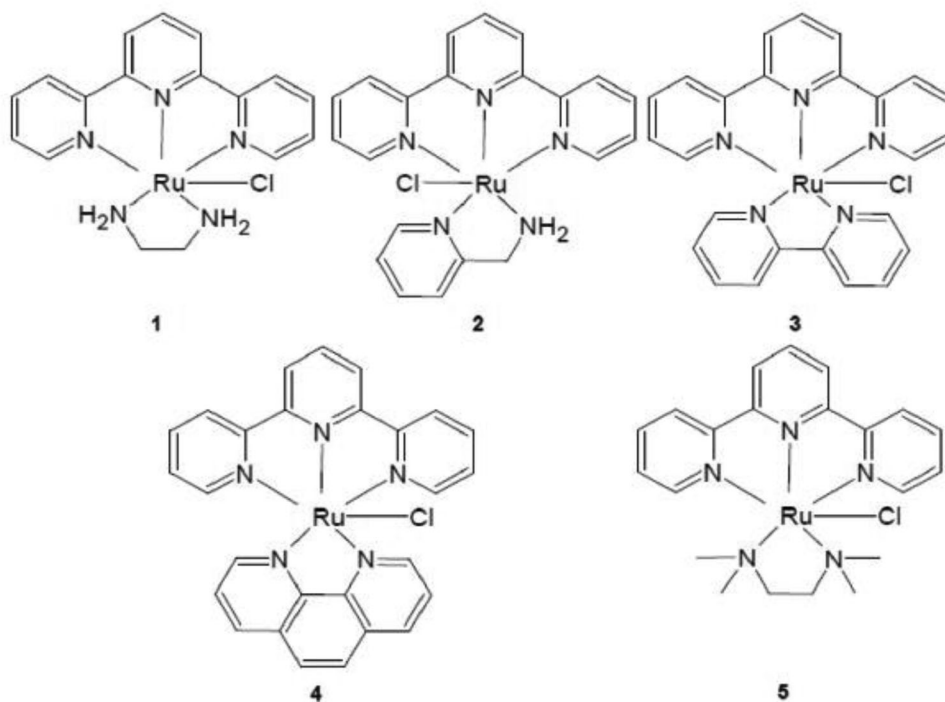


Figure 1. Schematic structures of the studied $[\text{Ru}^{\text{II}}(\text{terpy})(\text{N}^{\wedge}\text{N})\text{Cl}]^+$ complexes [1].

compared to DFT calculations in order to gain further insight into the underlying reaction mechanisms.

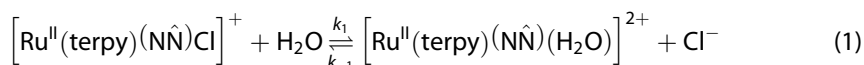
Quantum chemical methods

Optimization of the complex structures was performed using the hybrid functional B3LYP [5] in combination with the effective core potential def2svp [6], which is the commonly applied level of theory for such complexes [2, 3, 7]. All structures were characterized as local minima or true transition states by computation of vibration frequencies at the same level of theory (B3LYP/def2svp). To further evaluate the relative energies, ω B97XD [8]/def2tzvp [6] calculations were done on the B3LYP/def2svp structures, where the gained energies (ω B97XD/def2tzvp) were further ZPE-corrected (B3LYP/def2svp). All calculations were performed using GAUSSIAN09 suite of programs [9].

Results and discussion

At 37 °C, the spontaneous aquation reactions of the chlorido complexes **1–5** (Figure 1) were studied and found to be complete within 3.5 h, 2.4 h, 2.2 h, 30 min, and 2 min, respectively, i.e. $k_{\text{phen}} = (2.82 \pm 0.02) \times 10^{-4} \text{ s}^{-1}$, $k_{\text{bipy}} = (4.01 \pm 0.03) \times 10^{-4} \text{ s}^{-1}$, $k_{\text{tmén}} = (4.33 \pm 0.03) \times 10^{-4} \text{ s}^{-1}$, $k_{\text{ampy}} = (1.89 \pm 0.01) \times 10^{-3} \text{ s}^{-1}$, and $k_{\text{en}} = (2.45 \pm 0.04) \times 10^{-2} \text{ s}^{-1}$. At 25 °C, the aquation reactions were 4, 3.6, 3.6, 3, and 3.5 times slower, respectively. It follows that the reactivity of the Ru(II) chlorido complexes is strongly affected by electronic and steric factors of the spectator ligands. It increases with increasing number of pyridine rings coordinated to the metal center, i.e. with the π back-bonding ability of the spectator chelate. The data for the en and tmén complexes indicate a much higher stability of the latter one due to the steric hindrance provided by the bulky tmén ligand: phen > bipy \approx tmén > ampy > en [1–4].

The aquation reaction of the chlorido complexes can be fully reversed upon addition of an excess of chloride (Equation (1)). We found that the observed rate constants for the reformation of the chloride complexes are linear functions of the chloride concentration with intercepts indicating the reversibility of the studied reactions (see Figure 2). The slopes are the second-order rate constants for the anation of the aqua complexes by chloride, whereas the intercepts represent the first-order rate constants for the aquation of the chlorido complex as given by Equations (1) and (2).



$$k_{\text{obs}} = k_1 + k_{-1}[\text{Cl}^-] \quad (2)$$

The calculated k_1 , k_{-1} , and equilibrium constants $K (= k_1/k_{-1})$ for the reactions outlined in Equation (1) are reported in Table 1. Analysis of the data indicates that the rate constants k_1 and k_{-1} are significantly larger for the en and ampy complexes than for the other complexes. On the other hand, the reactivity of the tmén complex is similar to that of the bipy and phen complexes for both the aquation and anation

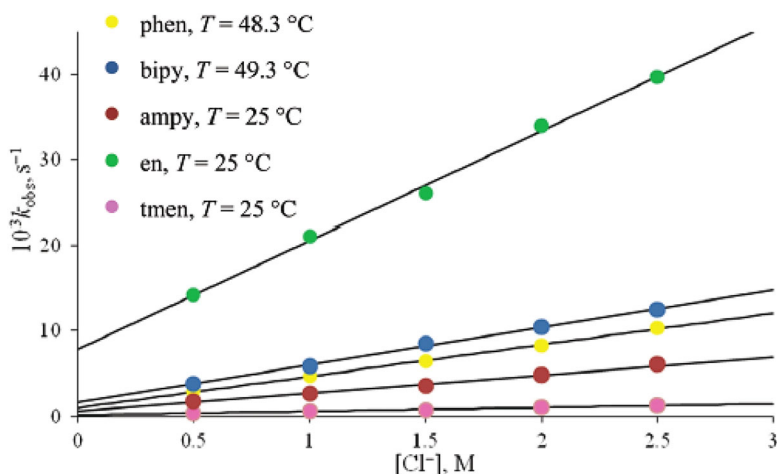


Figure 2. Plots of k_{obs} vs. $[\text{Cl}^-]$ for the reaction of $[\text{Ru}(\text{terpy})(\text{N}^{\wedge}\text{N})(\text{H}_2\text{O})]^{2+}$ with chloride; $I = 2.5 \text{ M}$ (Na^+ , NO_3^- , Cl^-) [1].

Table 1. $\text{p}K_a$ values, rate and equilibrium constants, and thermal activation parameters for aquation and anation reactions by Cl^- of $[\text{Ru}(\text{terpy})(\text{N}^{\wedge}\text{N})(\text{Cl}/\text{H}_2\text{O})]^{+2+}$ at 25°C [1].

System	$10^3 k_1 \text{ (s}^{-1}\text{)}$	$10^3 k_{-1} \text{ (M}^{-1} \text{s}^{-1}\text{)}$	$K \text{ (M)}$	$\text{p}K_a \text{ (} I = 0 \text{ M)}$	$\Delta H^\ddagger \text{ (kJ mol}^{-1}\text{)}$	$\Delta S^\ddagger \text{ (J K}^{-1} \text{mol}^{-1}\text{)}$
$[\text{en}-\text{Cl}] + \text{H}_2\text{O}$	7.0 ± 0.1	–	0.62 ± 0.03	–	–	–
$[\text{en}-\text{H}_2\text{O}] + \text{Cl}^-$	–	12.8 ± 0.4	–	10.83 ± 0.03	–	–
$[\text{ampy}-\text{Cl}] + \text{H}_2\text{O}$	0.64 ± 0.03	–	0.31 ± 0.03	–	–	–
$[\text{ampy}-\text{H}_2\text{O}] + \text{Cl}^-$	–	2.09 ± 0.08	–	10.36 ± 0.03	75 ± 3	-44 ± 11
$[\text{bipy}-\text{Cl}] + \text{H}_2\text{O}$	0.11 ± 0.01	–	0.26 ± 0.03	–	–	–
$[\text{bipy}-\text{H}_2\text{O}] + \text{Cl}^-$	–	0.42 ± 0.01	–	9.83 ± 0.03	78 ± 2	-46 ± 5
$[\text{phen}-\text{Cl}] + \text{H}_2\text{O}$	0.072 ± 0.001	–	0.20 ± 0.01	–	–	–
$[\text{phen}-\text{H}_2\text{O}] + \text{Cl}^-$	–	0.36 ± 0.01	–	9.59 ± 0.03	82 ± 2	-37 ± 6
$[\text{tmen}-\text{Cl}] + \text{H}_2\text{O}$	0.12 ± 0.01	–	0.28 ± 0.01	–	–	–
$[\text{tmen}-\text{H}_2\text{O}] + \text{Cl}^-$	–	0.43 ± 0.02	–	10.03 ± 0.02	79 ± 2	-44 ± 2

reactions. Furthermore, the higher K value for the en complex suggests that it aquates to a much higher degree than the other complexes.

The $\text{p}K_a$ values were determined using spectrophotometric pH titrations, and the obtained data are included in Table 1. The $[\text{Ru}(\text{terpy})(\text{N}^{\wedge}\text{N})(\text{H}_2\text{O})]^{2+}$ complexes are characterized by very high $\text{p}K_a$ values, varying from 9.59 to 10.83 with $[\text{Ru}(\text{terpy})(\text{phen})(\text{H}_2\text{O})]^{2+}$ and $[\text{Ru}(\text{terpy})(\text{en})(\text{H}_2\text{O})]^{2+}$ being the most and least acidic complexes, respectively [1]. Accordingly, under physiological conditions all examined $[\text{Ru}(\text{terpy})(\text{N}^{\wedge}\text{N})(\text{H}_2\text{O})]^{2+}$ complexes exist in their more reactive aqua form.

Analysis of the data in Table 1 reveals that the observed differences in acidic properties of the studied complexes are consistent with the difference in lability of the starting chlorido complexes. For instance, the water molecule is bound stronger to the Ru(II) center in the phen complex than in the en complex. Values of the equilibrium constant K (Equation (1)) are controlled by the efficiency of the forward (k_1) and back (k_{-1}) reactions. On the other hand, the efficiency of the back reaction (k_{-1}) correlates with the $\text{p}K_a$ values, which in turn increase with the lability of the coordinated water molecule. The data in Table 1 indicate that the reactivity and $\text{p}K_a$ values of the Ru(II)

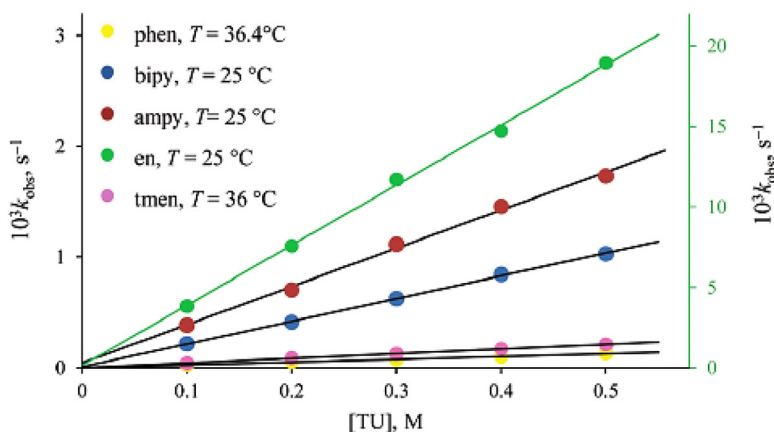


Figure 3. Plots of k_{obs} vs. [thiourea] for the anation reaction of the $[\text{Ru}(\text{terpy})(\text{N}^{\wedge}\text{N})(\text{H}_2\text{O})]^{2+}$ complexes; $I = 0.10 \text{ M}$ (Na^+ , NO_3^-) [1].

Table 2. Rate constants and activation parameters for substitution of the $[\text{Ru}(\text{terpy})(\text{N}^{\wedge}\text{N})(\text{H}_2\text{O})]^{2+}$ complexes by thiourea.

Complex	T ($^{\circ}\text{C}$)	$10^3 k_2$ ($\text{M}^{-1} \text{s}^{-1}$)	ΔH^{\ddagger} (kJ mol^{-1})	ΔS^{\ddagger} ($\text{J K}^{-1} \text{mol}^{-1}$)
[en- H_2O]	25	37.4 ± 0.1	65 ± 2	-55 ± 6
[ampy- H_2O]	25	3.57 ± 0.05	79 ± 1	-27 ± 4
[bipy- H_2O]	25	0.58 ± 0.02	83 ± 1	-29 ± 2
[phen- H_2O]	36.4	1.71 ± 0.04	79 ± 2	-43 ± 7
[tmen- H_2O]	36	2.89 ± 0.06	70 ± 2	-72 ± 7

complexes can systematically be tuned by variation of electronic and steric effects caused by the bidentate spectator chelates. As a consequence, the reactivity of the complexes increases in the order $\text{phen} \leq \text{bipy} \approx \text{tmen} < \text{ampy} < \text{en}$.

Being stimulated by the above results, we studied the reactions of the five aqua complexes with a bio-relevant nucleophile such as thiourea (TU). The studied ligand differs from chloride not only in its electronic charge, but also in its nucleophilicity based on the η_{Pt}^0 scale: $\text{Cl}^- < \text{TU}$ [10]. The reaction was studied as a function of thiourea concentration and plots of k_{obs} vs. thiourea concentration are linear with zero intercepts within the experimental error limits (see Figure 3), demonstrating the irreversibility of the reactions:

The second-order rate constant k_2 was calculated from the slope of the plots in Figure 3 since $k_{\text{obs}} = k_2[\text{TU}]$. Values of the second-order rate constants are summarized in Table 2 along with the activation parameters. In terms of a mechanistic interpretation, the activation entropy values reported in Tables 1 and 2 are all significantly negative and favor an associative interchange (I_a) substitution mechanism. Although the concept of an interchange mechanism is based on the formation of a precursor complex, kinetic evidence for the deviation of linearity on the k_{obs} versus nucleophile concentration plots was not observed in all the experimental work. This may be due to the fact that all reactions were studied in water for which precursor formation is expected to be weak.

To sum up, our experimental studies showed that the reactivity and acidity of the $[\text{Ru}(\text{terpy})(\text{N}^{\wedge}\text{N})(\text{Cl}/\text{H}_2\text{O})]^{+/2+}$ complexes can systematically be tuned by the nature of

the bidentate spectator ligand. Introduction of π -acceptors into the coordination sphere causes a decrease in electron density on the Ru(II) center and results in stronger coordination of the leaving monodentate ligand. This in turn, is reflected by the higher acidity of coordinated water as well as in the lower substitution reactivity of the complex. The pK_a values decrease with increasing number of pyridine rings surrounding the Ru(II) center: $en < ampy < tmen < bipy < phen$. Furthermore, the results demonstrate that the reactivity and pK_a values of the Ru(II) complexes can be tuned not only by electronic, but also by steric effects of the spectator bidentate ligands. In the case of four methyl substituents attached to the nitrogen atoms of the tmen ligand, it leads to significant deceleration of all substitution reactions of the tmen complex. In such a way, the reactivity of the tmen and bipy complexes toward entering ligands is very low. In general, rates of both the spontaneous aquation of the $[Ru^{II}(terpy)(N\wedge N)Cl]^+$ complexes and substitution of the coordinated water molecule in their aquated derivatives by chloride and thiourea increases in the following order: $[Ru^{II}(terpy)(phen)X]^{+/2+} < [Ru^{II}(terpy)(bipy)X]^{+/2+} \approx [Ru^{II}(terpy)(tmen)X]^{+/2+} < [Ru^{II}(terpy)(ampy)X]^{+/2+} < [Ru^{II}(terpy)(en)X]^{+/2+}$.

DFT calculations

To gain further insight at the molecular level for the mechanisms of water exchange and water substitution by thiourea, quantum chemical calculations were performed on the investigated complexes. Ground state optimization of the chlorido complexes **1–5** (Figure 1) resulted in structures of a quality and high comparability with the published X-ray data [2–4]. Comparison of the calculated (B3LYP/def2svp) structures of the investigated chlorido complexes **1–5**, with emphasis on the Ru-Cl bond distances, and the experimental X-ray data, reveals that the DFT calculated Ru-Cl bonds are consequently a bit longer (in general less than 0.1 Å) than the experimental structures, a trend also reported by Schramm *et al.* [7].

The water exchange reaction and the substitution of water by thiourea were studied by DFT calculations by constructing reaction paths for both processes as displayed in Figure 4. All energies were calculated relative to the reaction complex I (RC I). Reaction complex I is composed of the investigated complex and the entering nucleophile Y (H_2O or TU which was placed close to the leaving water molecule in the second coordination sphere). Starting with RC I, a transition state was calculated (TS) from which reaction complex II is formed during the displacement of a leaving water molecule by the entering nucleophile $Y=$ TU. No evidence for formation of either a five- or seven-coordinate intermediate, typical for a limiting dissociative (*D*) or associative (*A*) mechanism, was revealed by the DFT calculations. This is based on the fact that although we searched for such stable five- or seven-coordinate intermediates, we could not detect any and only found a single transition state for all studied reactions, i.e. solid evidence for an interchange mechanism.

All calculated energies for the species presented in Figure 4, along with bond distances of the metal center to the nucleophiles for the water exchange process and substitution of water by thiourea, are presented in Tables 3 and 4, respectively. In the case of a water exchange reaction in RC I, the entering water in the ground state is

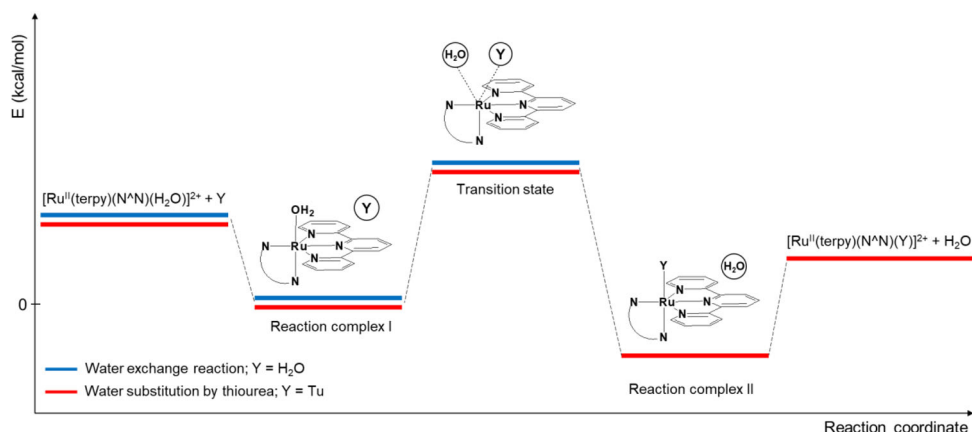


Figure 4. Reaction paths for water exchange and water substitution by thiourea for the studied aqua derivatives of 1–5 implemented in DFT calculations (for colors, see online version of the manuscript).

Table 3. Calculated energies (ω B97XD/def2tzvp//B3LYP/def2svp + ZPE(B3LYP/def2svp)) for the water exchange reactions of the aqua derivatives of 1–5 according to the reaction pathway presented in Figure 4.

Complex	E^a (kcal/mol)		d_e^d (Å)	d_1^e (Å)
	$Q^b + Y$	TS/Nimag ^c		
[en-H ₂ O]	15.40	19.34/1	3.04	3.31
[ampy-H ₂ O]	15.30	21.06/1	3.23	3.16
[bipy-H ₂ O]	15.04	20.40/1	3.27	3.13
[phen-H ₂ O]	14.92	20.37/1	3.11	3.24
[tmen-H ₂ O]	15.28	23.76/1	3.30	3.28

^aAll energies are relative to the formation of the reaction complex I.

^b $Q = [\text{Ru}^{\text{II}}(\text{terpy})(\text{N}^{\wedge}\text{N})(\text{H}_2\text{O})]^{2+}$.

^cNimag = Number of imaginary frequencies.

^dDistance between Ru^{II}-center and the oxygen of the entering water in the transition state.

^eDistance between Ru^{II}-center and the oxygen of the leaving water in the transition state.

Table 4. Calculated energies (ω B97XD/def2tzvp//B3LYP/def2svp + ZPE(B3LYP/def2svp)) for the substitution of water by thiourea for the aqua complexes of 1–5 according to the reaction pathway presented in Figure 4.

Complex	E^a (kcal/mol)					d_e^e (Å)	d_1^f (Å)
	$Q^b + Y$	TS/Nimag ^c	RC II	$Q^d + \text{H}_2\text{O}$			
[en-H ₂ O]	28.40	17.33/1	-4.40	4.43	3.39	3.06	
[ampy-H ₂ O]	26.20	19.34/1	-4.17	3.42	3.61	3.05	
[bipy-H ₂ O]	25.78	18.22/1	-0.56	3.94	3.71	3.25	
[phen-H ₂ O]	24.93	17.50/1	-1.56	2.90	3.68	3.22	
[tmen-H ₂ O]	26.95	18.62/1	-2.67	3.53	3.73	3.14	

^aAll energies are relative to the formation of a reaction complex I.

^b $Q = [\text{Ru}^{\text{II}}(\text{terpy})(\text{N}^{\wedge}\text{N})(\text{H}_2\text{O})]^{2+}$.

^cNimag = Number of imaginary frequencies.

^d $Q = [\text{Ru}^{\text{II}}(\text{terpy})(\text{N}^{\wedge}\text{N})(\text{Y})]^{2+}$, see Figure 4.

^eDistance between Ru^{II}-center and the sulfur of the entering thiourea in the transition state.

^fDistance between Ru^{II}-center and the oxygen of the leaving water in the transition state.

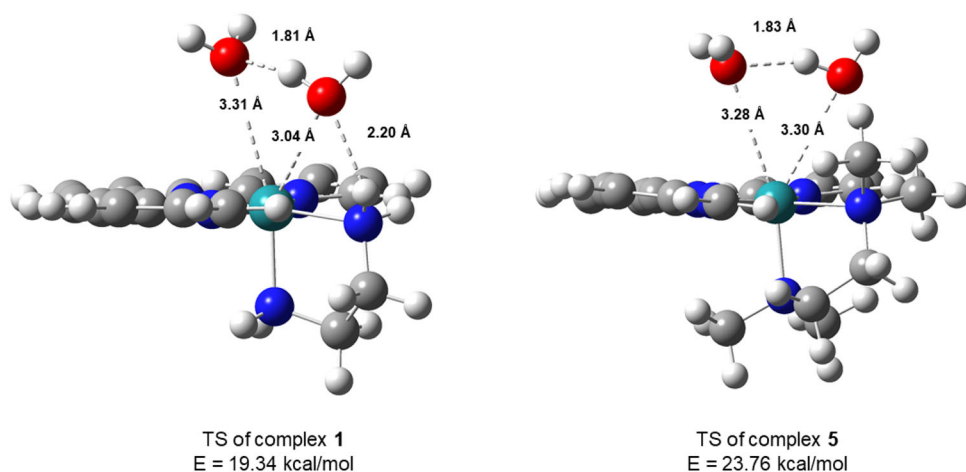


Figure 5. Calculated (B3LYP/def2svp) transition states for the water exchange reaction of aquated **1** and **5**, with the energy values relative to ω B97XD/def2tzvp//B3LYP/def2svp + ZPE(B3LYP/def2svp) and selected bond lengths.

placed in the second coordination sphere forming a hydrogen bond with the water molecule coordinated to the metal center. This arrangement of the entering water molecule results in formation of the relative symmetrical transition states, which are typical for an interchange (*I*) water exchange mechanism. However, this arrangement changes in the case of the aquated complex **1** in which the entering water molecule is located between the en ligand and the coordinated water molecule, most probably forming an additional hydrogen bond with the N-H group of the en ligand. The effect of this additional hydrogen bond can clearly be seen in the corresponding transition state. The distance of the entering water molecule to the Ru^{II} center (3.04 Å) is shorter than the distance of the leaving one (3.31 Å), which is in the end reflected in the transition state energy (Figure 5). For example, by comparison of the energy of the transition states of the aqua analogues of **1** and **5**, where complex **5** has no ability to form a similar type of additional hydrogen bond (Figure 5), the TS energy of aquated **1** is 4.42 kcal/mol lower. Thus, the ability to form an additional hydrogen bond with the inert spectator ligand of a complex close to the reaction center has a “slingshot” effect on the overall water exchange reaction.

Entrance of thiourea into the reaction system of the investigated aqua complexes is followed by a large stabilization of the system ranging from 24.9 to 28.4 kcal/mol. For all complexes except aqua complex **1**, thiourea approaches the Ru^{II} center from the site opposite to the chelate, similar to the case of the water exchange process discussed above. This type of thiourea approach is presented in Figure 6 compared to the approach from the opposite side of the chelating en ligand, which is disfavored by 2.43 kcal/mol. However, this particular approach of the entering thiourea has no significant effect on the transition state energy, or on the entering/leaving ligand bond distances to the Ru^{II} metal center (see Table 4) in comparison to the other investigated complexes. In all transition states of the investigated complexes, longer distances of the entering TU ligand compared to the leaving water molecule are observed. This may be related to the fact that thiourea is a bulky nucleophile such that it cannot

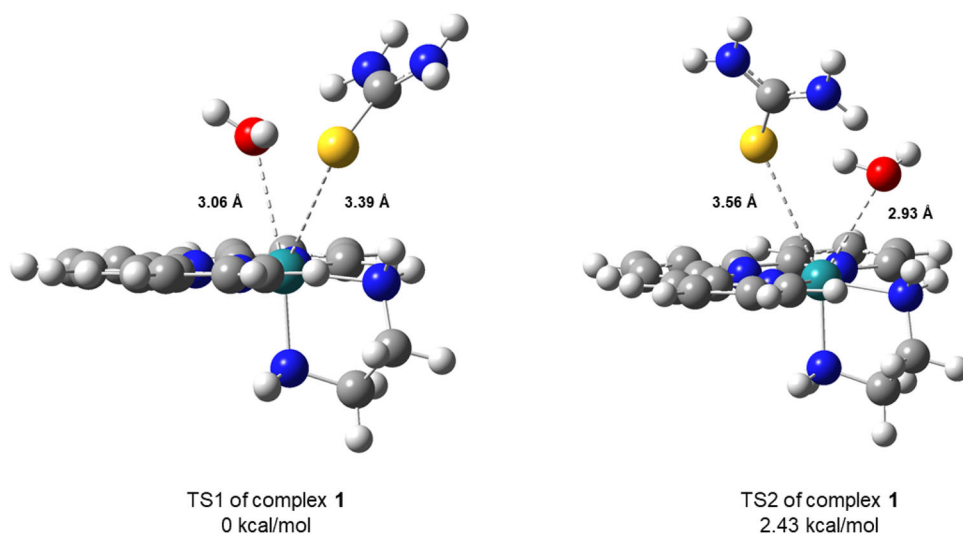


Figure 6. Transition states for different approaches of the entering thiourea ligand in the water displacement reaction of the aqua complex **1**, with selected bond lengths; the energy of TS2 is relative to the energy of TS1.

get as close to the metal center as an entering water molecule. The positions of the entering thiourea ligand in the transition state are such that significant bond formation has occurred, so that the nature of the underlying reaction mechanism can still be interpreted in terms of an associative interchange (I_a) mechanism. Following the transition state, a reaction complex II is formed in which thiourea is coordinated to the Ru^{II} metal center while the substituted water is located in the second coordination sphere. The ability of water to form a hydrogen bond is accompanied by a stabilization of -0.56 to -4.40 kcal/mol relative to its position inside the system.

For the reactions of the series of $[\text{Ru}^{\text{II}}(\text{terpy})(\text{N}^{\wedge}\text{N})(\text{H}_2\text{O})]^{2+}$ complexes with thiourea, the theoretical E_a values range from 19.3 to 23.8 kcal/mol compared to the experimental ΔH^\ddagger values for the same reactions that vary between 65 and 83 kJ/mol. It follows that the E_a values are somewhat higher than the ΔH^\ddagger values, something that is known for DFT calculations. However, these values do not differ too much and are within acceptable error limits.

Conclusion

The DFT computational studies have assisted in visualization of the transition state for both the water exchange and water displacement reactions by thiourea. The positions of the leaving and entering nucleophiles in the transition state are all within the range expected for a single transition state within the concept of an associative interchange (I_a) mechanism. The activation entropies reported in Tables 1 and 2 for the water exchange and water displacement reactions by thiourea, respectively, are in the range typical for an associative interchange (I_a) mechanism. In addition, volumes of activation (ΔV^\ddagger) for the reactions of **1** and **3** with thiourea, estimated from the slope ($= -\Delta V^\ddagger/RT$) of plots of $\ln k_{\text{obs}}$ vs. pressure, were -3.8 ± 0.5 and $-10 \pm 1 \text{ cm}^3 \text{ mol}^{-1}$ for the

en and bipy complexes, respectively [2]. The significantly negative values found for both the entropies and volumes of activation support the operation of an associative ligand substitution mechanism, most probably of the associative interchange (I_a) type, which is typical for substitution reactions of Ru(II) complexes [11].

Acknowledgments

We would like to thank Prof. Tim Clark and Prof. Wolfgang Hieringer for hosting this work at the CCC. The authors gratefully acknowledge the Regionales Rechenzentrum Erlangen (RRZE) for a generous allotment of computer time. D.Ć. thanks the Ministry of Education, Science and Technological Development of the Republic of Serbia (Agreement No. 451-03-68/2020-14/200122).

Disclosure statement

No potential conflict of interest was reported by the authors.

Funding

This project was supported financially by the National Science Center, Poland, Preludium, Grant No. 2019/33/N/ST4/0070.

ORCID

Ralph Puchta  <http://orcid.org/0000-0003-1370-3875>

References

- [1] C.D. Hubbard, D. Chatterjee, M. Oszajca, J. Polaczek, O. Impert, M. Chrzanowska, A. Katafias, R. Puchta, R. van Eldik. *Dalton Trans.*, **49**, 4599 (2020).
- [2] M. Chrzanowska, A. Katafias, O. Impert, A. Kozakiewicz, A. Surdykowski, P. Brzozowska, A. Franke, A. Zahl, R. Puchta, R. van Eldik. *Dalton Trans.*, **46**, 10264 (2017).
- [3] M. Chrzanowska, A. Katafias, A. Kozakiewicz, R. Puchta, R. van Eldik. *J. Coord. Chem.*, **71**, 1761 (2018).
- [4] M. Chrzanowska, A. Katafias, A. Kozakiewicz, R. van Eldik. *Inorg. Chim. Acta*, **504**, 119449 (2020).
- [5] (a) A.D. Becke. *J. Phys. Chem.*, **97**, 5648 (1993);(b) C. Lee, W. Yang, R.G. Parr. *Phys. Rev. B: Condens. Matter.*, **37**, 785 (1988);(c) P.J. Stephens, F.J. Devlin, C.F. Chabalowski, M.J. Frisch. *J. Phys. Chem.*, **98**, 11623 (1994).
- [6] F. Weigend, R. Ahlrichs. *Phys. Chem. Chem. Phys.*, **7**, 3297 (2005).
- [7] F. Schramm, V. Meded, H. Fliegl, K. Fink, O. Fuhr, Z. Qu, W. Klopffer, S. Finn, T.E. Keyes, M. Ruben. *Inorg. Chem.*, **48**, 5677 (2009).
- [8] J.D. Chai, M. Head-Gordon. *Phys. Chem. Chem. Phys.*, **10**, 6615 (2008).
- [9] M.J. Frisch, G.W. Trucks, H.B. Schlegel, G.E. Scuseria, M.A. Robb, J.R. Cheeseman, G. Scalmani, V. Barone, B. Mennucci, G.A. Petersson, M. Nakatsuji, X. Caricato, H.P. Li, A.F. Hratchian, J. Izmaylov, G. Bloino, J.L. Zheng, H. Sonnenberg, M. Hada, M. Ehara, K. Toyota, R. Fukuda, J. Hasegawa, M. Ishida, T. Nakajima, Y. Honda, O. Kitao, H. Nakai, T. Vreven, J.A. Montgomery, J.E. Peralta, Jr., F. Ogliaro, M. Bearpark, J.J. Heyd, E. Brothers, K.N. Kudin, V.N. Staroverov, T. Keith, R. Kobayashi, J. Normand, K. Raghavachari, A. Rendell, J.C.

Burant, S.S. Iyengar, J. Tomasi, M. Cossi, N. Rega, J.M. Millam, M. Klene, J.E. Knox, J.B. Cross, V. Bakken, C. Adamo, J. Jaramillo, R. Gomperts, R.E. Stratmann, O. Yazyev, A.J. Austin, R. Cammi, C. Pomelli, J.W. Ochterski, R.L. Martin, K. Morokuma, V.G. Zakrzewski, G.A. Voth, P. Salvador, J.J. Dannenberg, S. Dapprich, A.D. Daniels, O. Farkas, J.B. Foresman, J.V. Ortiz, J. Cioslowski, D.J. Fox. *Gaussian 09, Revision C.01*, Gaussian, Inc., Wallingford, CT (2010).

- [10] M.L. Tobe, J. Burgess. *Inorganic Reaction Mechanisms*, Addison-Wesley Longman, Harlow, England (1999).
- [11] L. Helm, A.E. Merbach. *Chem. Rev.*, **105**, 1923(2005).